

# Formation of $\eta'(958)$ -mesic nuclei and axial $U_A(1)$ anomaly at finite density

Hideko Nagahiro and Satoru Hirenzaki

Department of Physics, Nara Women's University, Nara 630-8506, Japan

(Dated: July 31, 2018)

We discuss the possibility to produce the bound states of the  $\eta'(958)$  meson in nuclei theoretically. We calculate the formation cross sections of the  $\eta'$  bound states with the Green function method for  $(\gamma, p)$  reaction and discuss the experimental feasibility at photon facilities like SPring-8. We conclude that we can expect to observe resonance peaks in  $(\gamma, p)$  spectra for the formation of  $\eta'$  bound states and we can deduce new information on  $\eta'$  properties at finite density. These observations are believed to be essential to know the possible mass shift of  $\eta'$  and deduce new information of the effective restoration of the chiral  $U_A(1)$  anomaly in the nuclear medium.

In the contemporary hadron physics, the light pseudoscalar mesons ( $\pi$ ,  $K$ ,  $\eta$ ) are recognized as the Nambu-Goldstone bosons associated with the spontaneous breaking of the QCD chiral symmetry. In real world, these mesons, together with heavier  $\eta'(958)$  meson, show the involved mass spectrum, which are believed to be explained by the explicit flavor  $SU(3)$  breaking due to current quark masses and the breaking of the axial  $U_A(1)$  symmetry at the quantum level referred as the  $U_A(1)$  anomaly [1, 2]. One of the most important subjects in hadron physics at present is to reveal the origin of the hadron mass spectra and to find out the quantitative description of hadron physics from QCD [3].

Recently, there are several very important developments for the study of the spontaneous breaking of chiral symmetry and its partial restoration at finite density. To investigate the in-medium behavior of spontaneous chiral symmetry breaking, the hadronic systems, such as pionic atoms [4, 5, 6],  $\eta$ -mesic nuclei [7, 8] and  $\omega$ -mesic nuclei [9], have been investigated in both of theoretical and experimental aspects. Especially, after a series of deeply bound pionic atom experiments [10, 11], K. Suzuki *et al.* reported the quantitative determination of pion decay constant  $f_\pi$  in-medium from the deeply bound pionic states in Sn isotopes [5] and stimulated many active researches of the partial restoration of chiral symmetry at finite density [4, 6, 12, 13, 14].

However, as for the behavior of the  $U_A(1)$  anomaly in the nuclear medium, the present exploratory level is rather poor. Although some theoretical results have been reported, there exists no experimental information on the possible effective restoration of the  $U_A(1)$  anomaly at finite density. T. Kunihiro studied the effects of the  $U_A(1)$  anomaly on  $\eta'$  properties at finite temperature using the Nambu-Jona-Lasinio model [15] with the KMT term [16, 17], which accounts for the  $U_A(1)$  anomaly effect, and showed the possible character changes of  $\eta'$  at  $T \neq 0$ . There is another theoretical work with a linear  $\sigma$  model [18]. Theoretical predictions by other authors also reported the similar consequences [19, 20] and supported the possible change of the  $\eta'$  properties at finite density as well as at finite temperature.

In this paper, we propose the formation reaction of

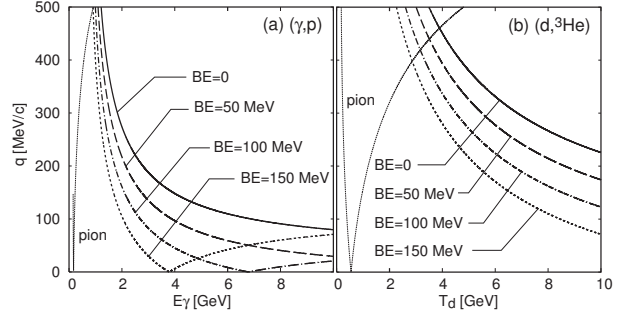


FIG. 1: Momentum transfer as functions of incident particle energies for the (a)  $(\gamma, p)$  and (b)  $(d, {}^3\text{He})$  reactions. Each line indicates the momentum transfer corresponding to the  $\eta'$ -mesic nucleus formation with different binding energy as shown in the figure. As for comparison, the momentum transfer for the pionic atom formation case is also shown.

the  $\eta'$ -mesic nuclei and discuss the possibility to produce the  $\eta'$ -nucleus bound states in order to investigate the  $\eta'$  properties, especially mass shift, at finite density. Since the huge  $\eta'$  mass is believed to have very close connection to the  $U_A(1)$  anomaly, the  $\eta'$  mass in the medium should provide us important information on the effective restoration of the  $U_A(1)$  symmetry in the nuclear medium.

In this study, we consider missing mass spectroscopy, which was proved to be a powerful tool for the meson bound states formation in the studies of deeply bound pionic states. In this spectroscopy, one observes only an emitted particle in a final state, and obtains the double differential cross section  $d^2\sigma/d\Omega/dE$  as a function of the emitted particle energy. In order to consider appropriate reaction for this system, we show momentum transfers as functions of incident particle energies for the  $(\gamma, p)$  and  $(d, {}^3\text{He})$  reactions in Fig. 1. The  $(d, {}^3\text{He})$  reaction has been used experimentally for the deeply bound pionic states formation [5, 10, 11, 21], and the  $(\gamma, p)$  reaction was proposed theoretically for the meson bound states formation [22, 23, 24]. As we can see from the figure, because of the large  $\eta'$  mass, we need to have larger incident energies than other meson formation cases to reduce the momentum transfer so as to have larger production rates. We think that the  $(\gamma, p)$  reaction with GeV photon

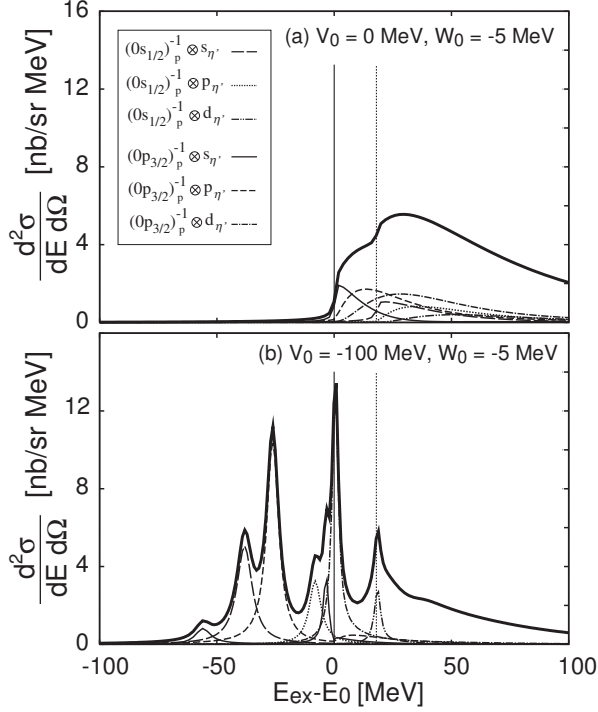


FIG. 2: The calculated spectra of  $^{12}\text{C}(\gamma, p)^{11}\text{B} \otimes \eta'$  reaction at  $E_\gamma = 3$  GeV are shown as functions of the excited energy  $E_{ex}$  defined in the text.  $E_0$  is the  $\eta'$  production threshold energy. The  $\eta'$ -nucleus optical potential are (a)  $V_0 = 0$ ,  $W_0 = -5$  MeV and (b)  $V_0 = -100$  MeV,  $W_0 = -5$  MeV. The total spectra are shown by the thick solid lines, and the dominant contributions of subcomponents are shown by dotted and dashed lines, as indicated in the figure. The vertical lines indicate the  $\eta'$  production threshold energy with the ground  $p_{3/2}$  proton-hole configuration (solid line) and the excited  $s_{1/2}$  proton-hole configuration (dotted line) in the final states.

beam is the appropriate reaction for our purpose since it can be performed in existing facilities like SPring-8. We adopt the  $(\gamma, p)$  reaction as a suitable one for the  $\eta'$ -mesic nuclei formation.

We choose the incident photon energy as  $E_\gamma = 3$  GeV, which is the beam energy accessible at SPring-8, and choose  $^{12}\text{C}$  as a target nucleus. We use the Green function method to calculate the formation cross sections [25] as,

$$\left( \frac{d^2\sigma}{d\Omega dE} \right)_{A(\gamma, p)\eta' \otimes (A-1)} = \left( \frac{d\sigma}{d\Omega} \right)_{p(\gamma, p)\eta'}^{\text{Lab}} \times \sum S(E), \quad (1)$$

where  $S(E)$  is the nuclear response function and  $\left( \frac{d\sigma}{d\Omega} \right)_{p(\gamma, p)\eta'}^{\text{Lab}}$  is the elementary cross section in the laboratory frame, which is estimated to be 150 nb/sr using the data of SAPHIR collaboration [26] and its analysis [27]. We sum up all (proton-hole) $\otimes$ ( $\eta'$ -particle) configurations to get the total cross section in Eq. (1).

To calculate the response function  $S(E)$ , we use the

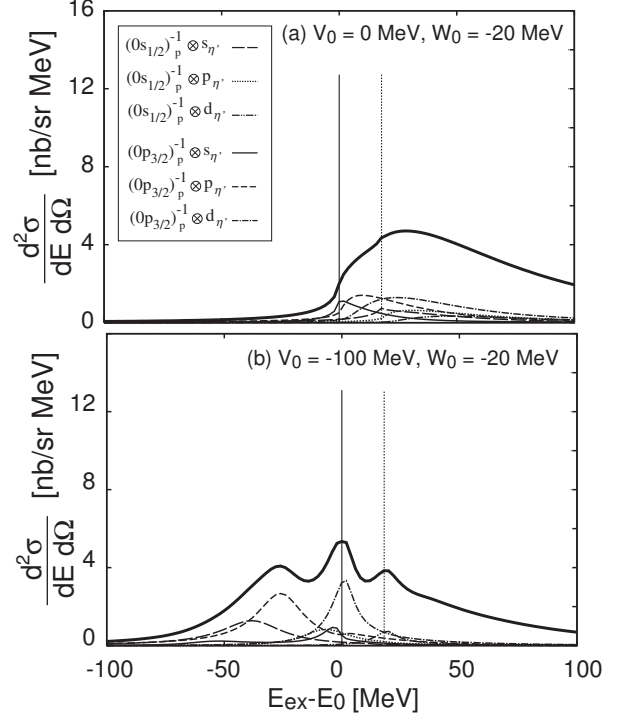


FIG. 3: The calculated spectra of  $^{12}\text{C}(\gamma, p)^{11}\text{B} \otimes \eta'$  reaction at  $E_\gamma = 3$  GeV are shown as functions of the excited energy  $E_{ex}$  defined in the text.  $E_0$  is the  $\eta'$  production threshold energy. The  $\eta'$ -nucleus optical potential are (a)  $V_0 = 0$ ,  $W_0 = -20$  MeV and (b)  $V_0 = -100$  MeV,  $W_0 = -20$  MeV. The total spectra are shown by the thick solid lines, and the dominant contributions of subcomponents are shown by dotted and dashed lines as indicated in the figure. The vertical lines indicate the  $\eta'$  production threshold energy with the ground  $p_{3/2}$  proton-hole configuration (solid line) and the excited  $s_{1/2}$  proton-hole configuration (dotted line) in the final states.

Green function  $G(E; \mathbf{r}, \mathbf{r}')$  defined as [25],

$$G(E; \mathbf{r}, \mathbf{r}') = \langle p^{-1} | \phi_{\eta'}(\mathbf{r}) \frac{1}{E - H_{\eta'} + i\epsilon} \phi_{\eta'}^\dagger(\mathbf{r}') | p^{-1} \rangle, \quad (2)$$

where  $\phi_{\eta'}^\dagger$  is the  $\eta'$  creation operator and  $|p^{-1}\rangle$  is a proton hole state. The Hamiltonian  $H_{\eta'}$  contains the  $\eta'$ -nucleus optical potential  $U$ . We can rewrite Eq. (2) in a simple expression as,

$$G(E; \mathbf{r}, \mathbf{r}') = \sum_{l_{\eta'}, m_{\eta'}} Y_{l_{\eta'}, m_{\eta'}}^*(\hat{r}) Y_{l_{\eta'}, m_{\eta'}}(\hat{r}') G_{l_{\eta'}}(E; r, r') \quad (3)$$

$$G_{l_{\eta'}}(E; r, r') = -2m_{\eta'} k u_{l_{\eta'}}(k, r_<) v_{l_{\eta'}}^{(+)}(k, r_>), \quad (4)$$

where  $u_{l_{\eta'}}$  and  $v_{l_{\eta'}}^{(+)}$  respectively are the radial part of the regular and outgoing solutions of equation of motion. Using the Green function, the response can be calculated

as

$$S(E) = -\frac{1}{\pi} Im \sum_{M, m_s} \int d^3r d\sigma d^3r' d\sigma' f^\dagger(\mathbf{r}, \sigma) G(E; r, r') f(\mathbf{r}', \sigma). \quad (5)$$

We define  $f(\mathbf{r}, \sigma)$  as

$$f(\mathbf{r}, \sigma) = \chi_f^*(\mathbf{r}) \xi_{\frac{1}{2}, m_s}^*(\sigma) \left[ Y_{\eta'}^*(\hat{r}) \otimes \psi_{j_p}(\mathbf{r}, \sigma) \right]_{JM} \chi_i(\mathbf{r}), \quad (6)$$

where  $\chi_i$  and  $\chi_f$  respectively denote the projectile and the ejectile distorted waves,  $\psi$  is the proton hole wavefunction and  $\xi$  is the spin wavefunction introduced to count possible spin directions of the proton in the target nucleus. The numerical values of  $S(E)$  were evaluated by using the eikonal approximation as in Ref. [28].

The  $\eta'$ -nucleus optical potential  $V(r)$  is assumed to have the following form as,

$$U(r) = (V_0 + iW_0) \frac{\rho(r)}{\rho_0}, \quad (7)$$

where  $\rho(r)$  is the nuclear density distribution and  $\rho_0$  denotes the nuclear saturation density. We treat  $V_0$  as a parameter and estimate its reasonable running range using the theoretical evaluation of the  $\eta'$  mass shift at  $\rho_0$  as  $V_0 = 0 \sim -150$  MeV [15, 19, 20]. We estimate the imaginary strength  $W_0$  from analysis of  $\gamma p \rightarrow \eta' p$  data [29]. Since they included only  $N^*(1535)$  as a baryon resonance in the analysis of the  $\eta'$  formation reaction and determined  $\eta' NN^*(1535)$  coupling strength, we can easily calculate the  $\eta'$  self-energy in the medium in analogy with the  $\Delta$ -hole model for the  $\pi$ -nucleus system as,

$$U \sim \frac{g^2}{2m_{\eta'} m_{\eta'} + M_N - M_{N^*} + i\Gamma_{N^*}/2} \frac{\rho}{\rho_0} = (+77 - 8i) \frac{\rho}{\rho_0} [\text{MeV}]. \quad (8)$$

We use the values as  $-5$  MeV and  $-20$  MeV for the imaginary part  $W_0$  based on this evaluation in Eq. (8). We should mention here that the evaluation in Eq. (8) provides the repulsive real part which is opposite to the evaluation from the  $\eta'$  mass shift. If the real potential is repulsive, we do not have any peak structure in the  $(\gamma, p)$  spectra due to the bound state formation. By the  $(\gamma, p)$  experiments proposed in this paper, we can expect to distinguish these potentials and to determine the sign and strength of the  $\eta'$ -nucleus optical potential.

In Fig. 2 and 3, we show the calculated spectra as functions of the excited energy which are defined as,

$$E_{ex} = m_{\eta'} - B_{\eta'} + [S_p(j_p) - S_p(p_{3/2})], \quad (9)$$

where  $B_{\eta'}$  is the  $\eta'$  binding energy and  $S_p$  the proton separation energy. The  $\eta'$  production threshold energy  $E_0$  is indicated in the figure by the vertical solid lines.

We calculate four cases with  $V_0 = 0$  and  $W_0 = -5$  MeV in Fig. 2(a),  $V_0 = -100$  MeV and  $W_0 = -5$  MeV in Fig. 2(b),  $V_0 = 0$  and  $W_0 = -20$  MeV in Fig. 3(a), and  $V_0 = -100$  MeV and  $W_0 = -20$  MeV in Fig. 3(b), in order to simulate the sensitivities of the reaction spectra to the complex potential strength within the reasonable parameter range discussed above.

As we can see from these figures, we can expect to observe the peak structure in the spectra due to the formation of the  $\eta'$ -mesic nucleus even in the case with the strong imaginary potential (Fig. 3), and we can expect to deduce the magnitude of the  $\eta'$  mass shift at finite nuclear density from the observed spectra. The evaluated imaginary part of the  $\eta'$ -nucleus potential is small enough and the resonance peaks are expected to be clearly separated each other. The absolute magnitude of the formation cross section is reasonably large and the spectra expected to be observed in experiments at SPring-8 [30].

The present evaluation is the first theoretical results for the formation of the  $\eta'$ -mesic nuclei to know the behavior of  $U_A(1)$  anomaly in the medium. We believe that the present theoretical results is much important to stimulate both theoretical and experimental activities to study the  $U_A(1)$  anomaly at finite density and to obtain the deeper insights of QCD symmetry breaking pattern and the meson mass spectrum.

We would like to thank for D. Jido, T. Hatsuda, A. Hosaka, T. Kunihiro, M. Oka, and M. Takizawa for useful comments and discussions.

- 
- [1] T. Kunihiro and T. Hatsuda, Phys. Lett. B **206**, 385 (1988), Erratum *ibid.* **210**, 278 (1988).
  - [2] V. Bernard, R. L. Jaffe and U. -G. Meissner, Nucl. Phys. B **308**, 753 (1988).
  - [3] For reviews; T. Hatsuda and T. Kunihiro, Phys. Rep. **247**, 221 (1994), and references therein.
  - [4] P. Kienle, and T. Yamazaki, Phys. Lett. B **514**, 1 (2001); H. Geissel, *et al.*, *ibid.* **549**, 64 (2002).
  - [5] K. Suzuki *et al.*, Phys. Rev. Lett. **92**, 072302 (2004).
  - [6] E.E. Kolomeitsev, N. Kaiser, and W. Weise, Phys. Rev. Lett. **90**, 092501 (2003).
  - [7] D. Jido, H. Nagahiro, and S. Hirenzaki, Phys. Rev. C **66**, 045202 (2002); H. Nagahiro, D. Jido and S. Hirenzaki, *ibid.* **68**, 035205 (2003).
  - [8] C. Garcia-Recio, J. Nieves, T. Inoue, and E. Oset, Phys. Lett. B **550**, 47 (2002); T. Inoue and E. Oset, Nucl. Phys. A **710**, 354 (2002).
  - [9] F. Klingl, T. Waas, and W. Weise, Nucl. Phys. **A650**, 299 (1999).
  - [10] H. Gilg *et al.*, Phys. Rev. C **62**, 025201 (2000); K. Itahashi *et al.*, *ibid.* C **62**, 025202 (2000).
  - [11] H. Geissel *et al.*, Phys. Rev. Lett. **88**, 122301 (2002).
  - [12] C. Garcia-Recio, J. Nieves and E. Oset, Phys. Lett. B **541**, 64 (2002).
  - [13] G. Chanfray, M. Ericson and M. Oertel, Phys. Lett. B **563**, 61 (2003).

- [14] E. Friedman and A. Gal, Phys. Lett. B **578**, 85 (2004).
- [15] T. Kunihiro, Phys. Lett. B **219**,363 (1989).
- [16] M. Kobayashi and T. Maskawa, Prog. Theor. Phys. **44**, 1422 (1970); M. Kobayashi, H. Kondo and T. Maskawa, Prog. Theor. Phys. **45**, 1955 (1971).
- [17] G. 't Hooft, Phys. Rev. D **14**, 3432 (1976), Phys. Rep. **142**, 357 (1986); M. A. Shifman, A.I. Vainshtein and V.Z. Zakharov, Nucl. Phys. **B163**, 46 (1980).
- [18] R.D. Pisarski and F. Wilczek, Phys. Rev. D **29**, 338 (1984).
- [19] K. Fukushima, K. Ohnishi, and K. Ohta, Phys. Rev. C **63**, 045203 (2001).
- [20] P. Costa, M.C. Ruivo, Yu. L. Kalinovsky, Phys. Lett. B **560**, 171 (2003); P. Costa, M.C. Ruivo, C.A. de Sousa, Yu. L. Kalinovsky, hep-ph/0408177.
- [21] S. Hirenzaki, H. Toki and T. Yamazaki, Phys. Rev. C **44**, 2472 (1991).
- [22] E. Marco and W. Weise, Phys. Lett. B **502**, 59 (2001).
- [23] S. Hirenzaki and E. Oset, Phys. Lett. B **527**, 69 (2002).
- [24] H. Nagahiro, D. Jido and S. Hirenzaki, in preparation.
- [25] O. Morimatsu and K. Yazaki, Nucl. Phys. **A435**, 727 (1985); **A483**, 493 (1988).
- [26] SAPHIR Collaboration, Phys. Lett. B **444**, 555 (1998).
- [27] W.T. Chiang, S.N. Yang, L. Tiator, M. Vanderhaeghen, and D. Drechsel, Phys. Rev. C **68**, 045202 (2003).
- [28] R.S. Hayano, S. Hirenzaki and A. Gillitzer, Eur. Phys. J. A **6**, 99 (1999).
- [29] A. Sibirtsev, Ch. Elster, S. Krewald and J. Speth, nucl-th/0303044.
- [30] N. Muramatsu, in private communication.